

Investigation of vortex lattices in a high-temperature superconductor by the EPR decoration technique

A. A. Koshta, Yu. N. Shvachko, A. A. Romanyukha, and V. V. Ustinov

Institute of Metal Physics, Ural Division of the Russian Academy of Sciences, 620219, Ekaterinburg, Russia

(Submitted 18 August 1992)

Zh. Eksp. Teor. Fiz. **103**, 629–654 (February 1993)

Results are presented of EPR studies carried out on the superconducting ceramics $\text{YBa}_2\text{Cu}_3\text{O}_7$ and $\text{Tl}_2\text{Ba}_2\text{Ca}_2\text{Cu}_3\text{O}_{10}$ and on single crystals of $\text{YBa}_2\text{Cu}_3\text{O}_7$ coated (decorated) with the organic radical DPPH, which possesses a narrow EPR line. Inhomogeneous broadening of the DPPH line caused by the vortex lattice was observed for all samples below T_c . The value of the magnetic penetration depth λ_0 and the behavior of $\lambda(T)$ were extracted from the temperature dependence of the EPR linewidth. The values of λ_0 obtained were 3900 Å for $\text{Tl}_2\text{Ba}_2\text{Ca}_2\text{Cu}_3\text{O}_{10}$, 3500 Å for $\text{YBa}_2\text{Cu}_3\text{O}_{7-\delta}$, and 1200 Å for the single crystals of $\text{YBa}_2\text{Cu}_3\text{O}_{7-\delta}$ they are satisfactorily described by the law $[1 - (T/T_c)^4]^{-1/2}$. The experiments with single crystals of $\text{YBa}_2\text{Cu}_3\text{O}_{7-\delta}$ confirm that vortex-lattice irregularities give the main contribution to the EPR linewidth below T_c and not shielding effects.

1. INTRODUCTION

Since the very moment of the discovery of high-temperature superconducting compounds a multitude of experiments have been carried out with the goal of obtaining accurate values of the superconducting parameters, in particular, the penetration depth of the magnetic field $\lambda(T)$. However, the data which have been obtained depend strongly on the mode of preparation of the sample and on the measurement technique employed.

The experimental values of λ_0 have a significant spread: for La–Sr–Cu–O—from 2500 to 6500 Å (Refs. 1–3), for Y–Ba–Cu–O—from 200 to 8000 Å (Refs. 4–11), for Bi–Sr–Ca–Cu–O—3500 Å (Ref. 12), for Tl–Ba–Cu–O—1700 Å (Ref. 13).

On the basis of the physics involved, techniques for determining λ can be divided into two categories: bulk-sensitive and locally sensitive. In the present paper we will be interested mainly in locally sensitive techniques such as μ^+ SR, NMR, and polarized neutron scattering. These techniques are based on the measurement of some physical parameters that are sensitive to local bulk magnetic fields that arise as a consequence of the existence of vortex lattices.^{14–18} Other techniques, such as static magnetization¹¹ and dynamic susceptibility,^{7,19} although not local, are nevertheless sensitive to the distribution of the vortex lattice inside the sample and can give information about the penetration depth.

The list of presently existing methods of measuring the vortex lattice parameters has recently by the addition of a new technique—the “decoration” of the surface of the superconductor by a material possessing a narrow EPR signal.^{20–26} The idea of this method is the following: the existence of the Abrikosov vortex lattice, which arises inside the superconducting sample at temperatures below T_c , leads to the appearance of local magnetic fields both in the bulk of the superconductor and on its surface. Deposition of an EPR probe on the sample surface makes it possible to record these local fields via inhomogeneous broadening of the signal from this probe. As the EPR probe it is necessary to use a material with a sufficiently narrow signal (in units of oersteds) whose

width depends weakly on temperature. In this case, the temperature dependence of the parameters of the EPR signal will contain information about the parameters of the vortex lattice and, in particular, the magnetic penetration depth λ .

The nature of the magnetic field density distribution $n(B)$ on the surface of a type-II superconductor has been studied in detail.^{27–29} It was shown that for a semi-infinite superconductor $n(B)$ has a maximum whose position is determined by the superconducting parameters B_{c2} and λ_0 and the value of the external magnetic field B .^{28,29} However, the shape of $n(B)$ becomes more complicated due to irregularities in the vortex lattice: pinning effects, distortions, etc.^{23,29}

It soon became clear that the experimental results demanded more careful mathematical treatment, one which takes account of inhomogeneous diamagnetic screening and intergranular field penetration.^{20–22}

Another problem arises for finite-size samples. In the decoration of the ceramic samples the EPR probe is deposited over their entire surface. As a result, in the geometry of the experimental all of the possible orientations of the decorated surfaces relative to the external magnetic field are obtained. Depending on the orientation, the shift of the resonance field strength can be either positive or negative. Moreover, the value of the shift depends strongly on the thickness of the sample.²⁰

In the present paper we present results of a further development of the technique of recording vortex lattices by decorating the surface of the sample with an EPR probe. A technique of local decoration of single-crystal samples is proposed which allows one to avoid some of the difficulties that have so far dogged the interpretation of the experimental results. Decoration of the ab surface makes it possible to determine the value of λ_1 .

2. EXPERIMENTAL METHOD AND SAMPLE PREPARATION

The EPR spectra were recorded with standard homodyne ERS-230 and ERS-231 X-band spectrometers. Computer processing of the spectra was used to accumulate signal data by repeated passage through the resonance conditions and accurately determine the parameters of the

TABLE I. Parameters of the investigated samples.

Parameters	YBa ₂ Cu ₃ O ₇ ceramic	YBa ₂ Cu ₃ O ₇ single crystal	Tl ₂ Ba ₂ Ca ₂ Cu ₃ O ₁₀ ceramic
$a, \text{\AA}$	3,823	3,817	3,851
$c, \text{\AA}$	11,670	11,684	35,621
T_c, K	94	92	122
$\Delta T_c, \text{K}$	2	0,1*	10**
$\chi \cdot 10^4, \text{mole}^{-1}$	3,0	—	3,1
$\rho, \text{m}\Omega \cdot \text{cm}$	0,40	—	3 — 8
$\rho_{ab}, \text{m}\Omega \cdot \text{cm}$	—	0,18	—
$\rho_c, \text{m}\Omega \cdot \text{cm}$	—	23***	—

*The value of ΔT_c was determined from the dependence of $\rho_{ab}(T)$ with a measurement current of 10 μA .

**A small tail in the temperature dependence of the static magnetic susceptibility was observed down to 100 K.

***The dependence $\rho_c(T)$ displayed a metallic character.

EPR line. The temperature of the samples was set and stabilized by an Oxford Instruments ESR 900 continuous-flow helium cryostat in which temperatures could be maintained in the range 3.5–300 K with an accuracy of 0.1 K.

The investigations were carried out on the superconducting ceramics YBa₂Cu₃O₇ and Tl₂Ba₂Ca₂Cu₃O₁₀ and single crystals YBa₂Cu₃O_{7- δ} . Values of the lattice parameters a and c , the transition temperature T_c , the transition width ΔT_c (measured between the 0.1 and 0.9 levels of the dynamic susceptibility), and some other parameters are given in Table I.

The YBa₂Cu₃O₇ samples were synthesized at the Institute of Metal Physics, Ural Division of the Russian Academy of Sciences,³⁰ and the ceramic Tl₂Ba₂Ca₂Cu₃O₁₀ was prepared in the Institute of Solid State and Semiconductor Physics of the Belorussian Academy of Sciences. The single crystals of YBa₂Cu₃O_{7- δ} (dimensions 0.05 × 2 × 3 mm³) were annealed in an O₂ atmosphere at 500 °C for 100 h. The superconducting properties of the samples were investigated by the microwave hysteresis technique both before and after decoration. A detailed description of this technique can be found elsewhere.³¹⁻³³ As the EPR probe we used a finely dispersed powder of the organic radical diphenyl-picrilhydrazil (DPPH) with ΔH (300 K) \leq 2 Oe.

The ceramic samples was decorated using three different techniques: grinding of the sample together with the finely dispersed DPPH powder, crystallization of the DPPH on the surface from a concentrated solution in acetone, and deposition onto the surface from a suspension of DPPH in ethanol. Single-crystal samples were decorated by crystallization and by deposition of DPPH onto one of the frontal planes of the crystal. Afterward, the samples were kept in open air until the acetone or ethanol evaporated. Deposition and evaporation were monitored with an optical microscope with 20 × magnification.

3. EXPERIMENTAL RESULTS

The width of the EPR line of DPPH (see Fig. 1) is practically independent of temperature for $T > 20$ K ($\Delta B \approx 2$ Oe), but at lower temperatures it becomes substantial. Over the entire temperature range the linewidth can be accurately fitted by the expression

$$\Delta B(T) = \frac{\Delta B(300 \text{ K})}{\sqrt{T}} \sqrt{300}. \quad (1)$$

Here the resonance field $B_r(T)$ is constant and equal to 3371.6 Oe ($g = 2.0043$).

Note that in contrast to the results obtained in Ref. 22, we did not observe a “step” in the dependence of $\Delta B(T)$ below $T = 240$ K for the signal from the DPPH deposited on the surface of the ceramic and single-crystal samples, and the linewidth was five times smaller than reported in Ref. 22. Apparently, the step-like feature noted above was an individual property of the sample used in Ref. 22.

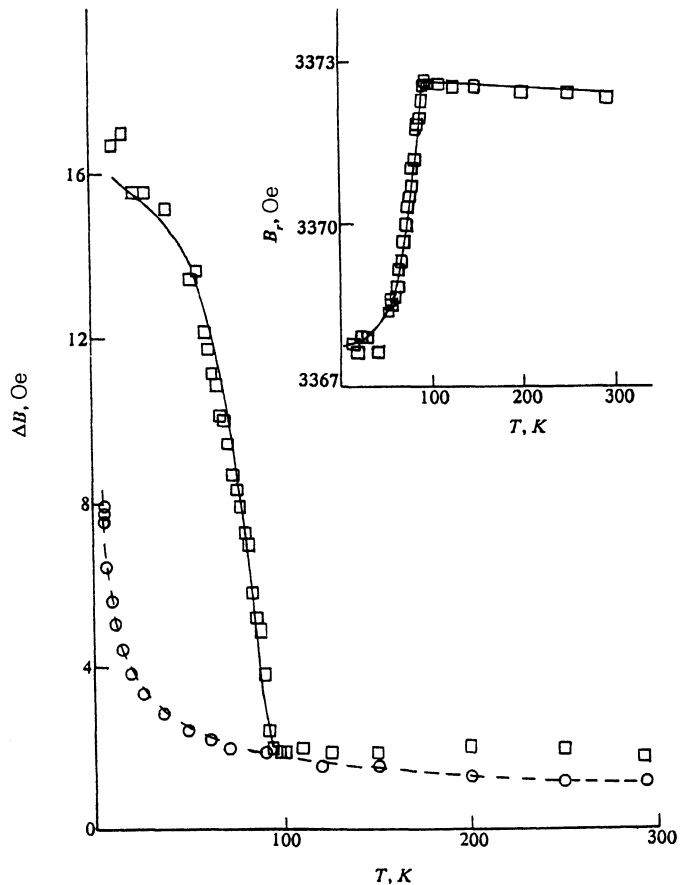


FIG. 1. Temperature dependences of the EPR linewidth of pure DPPH powder (O) and of a sample of the ceramic YBa₂Cu₃O_{7- δ} decorated with DPPH (□). Inset: temperature dependence of the resonance field of the EPR signal for a sample of the ceramic YBa₂Cu₃O_{7- δ} .

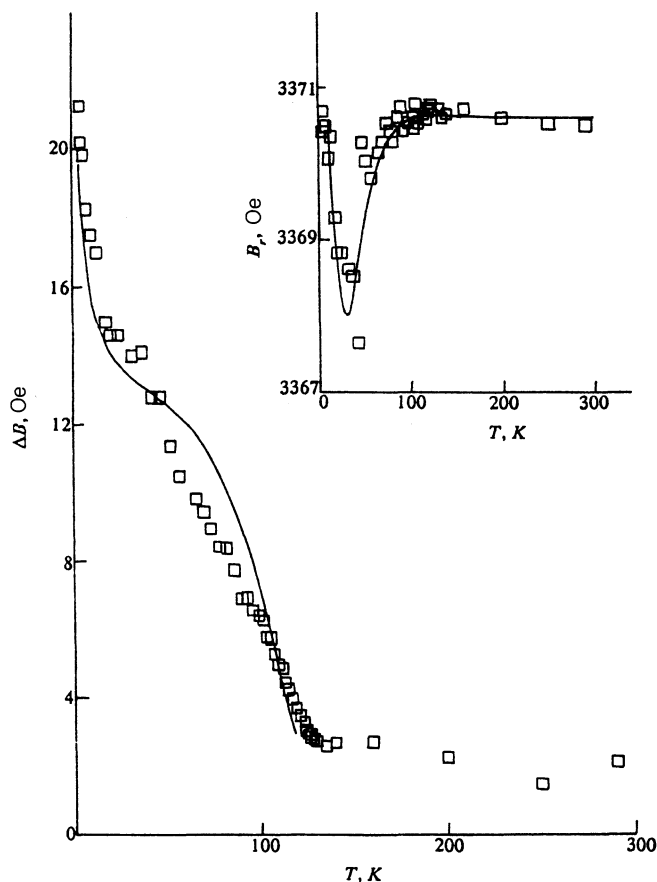


FIG. 2. Temperature dependence of the EPR linewidth of a sample of the ceramic $\text{Tl}_2\text{Ba}_2\text{Ca}_2\text{Cu}_3\text{O}_{10}$ decorated with DPPH. Inset: temperature dependence of the resonance field of the EPR signal for a sample of the ceramic $\text{Tl}_2\text{Ba}_2\text{Ca}_2\text{Cu}_3\text{O}_{10}$.

As has been already stated, we used three different techniques for depositing DPPH onto the surface of the ceramic sample. The greatest amplitude of the EPR signal from the DPPH was obtained for samples prepared by mechanical grinding, since this technique introduces the largest number of paramagnetic centers. A shortcoming of this technique is poor mechanical contact between the grains of the ceramic sample and the DPPH particles. The method of deposition of the finely dispersed powder from ethanol suffered from this same shortcoming. The method of crystallization provided the best contact of the paramagnetic centers with the sample surface. However, in order to compare these values of λ_0 and $\lambda(T)$, we present results here for samples prepared by all three methods.

Measured values of the EPR linewidth and the resonance field of the DPPH deposited on the surface of the ceramic samples of $\text{YBa}_2\text{Cu}_3\text{O}_7$ and $\text{Tl}_2\text{Ba}_2\text{Ca}_2\text{Cu}_3\text{O}_{10}$ are plotted in Figs. 1 and 2 as functions of temperature. The measured total intensity for both samples show Curie temperature dependence in the temperature region above T_c followed by a small plateau in the temperature range between T_c and 40 K, followed again by Curie-like behavior down to the lowest temperatures, but now with a different Curie constant. We assume that the change in the behavior of the total intensity below T_c reflects the exclusion of the paramagnetic centers that penetrated into the bulk of the sample during decoration from absorption of the microwave field due to

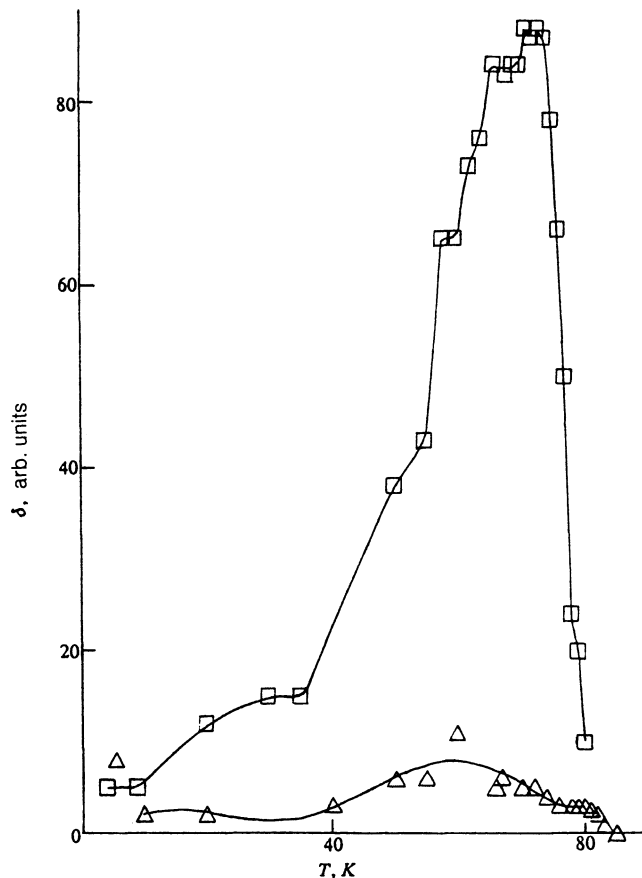


FIG. 3. Temperature dependence of the hysteresis amplitude for a single-crystal sample of $\text{YBa}_2\text{Cu}_3\text{O}_{7-\delta}$ for perpendicular (\square) orientation of the external magnetic field relative to the crystal plane, and parallel (\triangle).

shielding by the superconducting surface. This effect can be used to verify the quality of deposition of the EPR probe. The closer the temperature dependence of the intensity is to a Curie law, the better the quality of decoration of the sample, i.e., the fewer paramagnetic centers have penetrated into the bulk of the sample.

Figures 1 and 2 show an abrupt growth of the EPR linewidth observed for $\text{YBa}_2\text{Cu}_3\text{O}_7$ below $T_c = 93$ K and for $\text{Tl}_2\text{Ba}_2\text{Ca}_2\text{Cu}_3\text{O}_{10}$ below $T_c = 122$ K. This behavior of the linewidth, like the shift of the EPR line below these temperatures toward weaker fields, is due to the appearance of a vortex lattice in the bulk of the superconducting sample. The appearance of a monotonic shift of the EPR line below T_c is consistent with this assumption.

No EPR signals associated with nonsuperconducting phases were observed for any of the ceramic samples.³⁴ In the recording of the signal in fields from 1 to 5 kOe, hysteresis of microwave absorption was observed in the superconducting state. This effect consists of a jump in the level of microwave absorption when the magnetic field reverses. The magnitude of the jump is called the hysteresis amplitude, which has been discussed in more detail in Refs. 31–33.

Typical temperature behavior of the hysteresis amplitude for single-crystal samples is shown in Fig. 3. It is in agreement with the results of Ref. 35. The width of the maximum in this dependence is connected with microwave losses in the single crystals and characterizes the quality of the sample.^{35,36} We also observed that the position of this maxi-

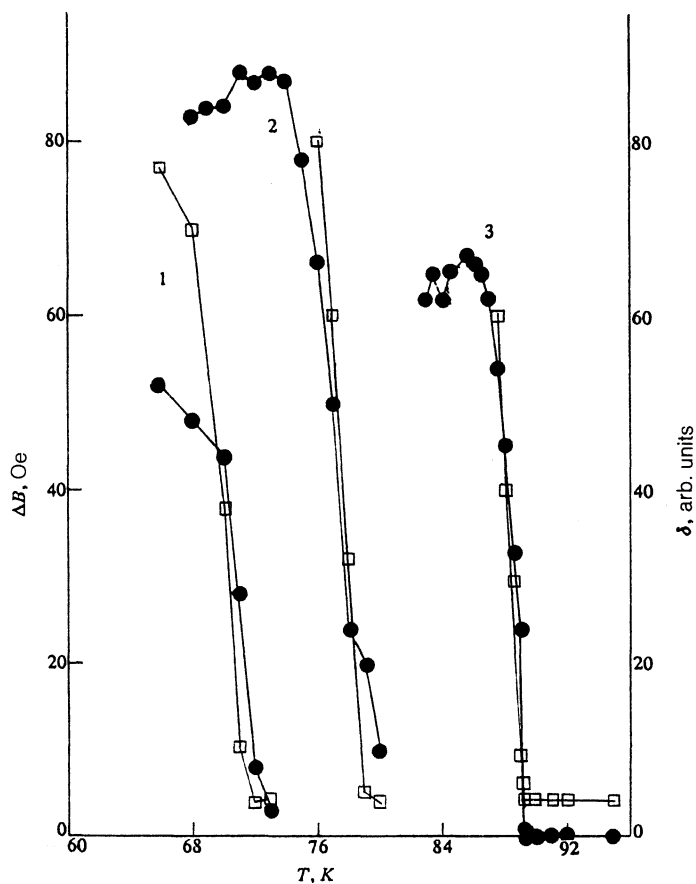


FIG. 4. Temperature dependence of the hysteresis amplitude (●) and EPR linewidth (□) for single-crystal samples of $\text{YBa}_2\text{Cu}_3\text{O}_{7-\delta}$ after decoration (1), after two days (2), and after a week (3).

imum is shifted closer to T_c for more ideal samples, which is in agreement with the results of Ref. 36. The temperature dependence of the hysteresis amplitude of the microwave absorption, obtained in the temperature range between the maximum and T_c , is shown in Fig. 4.

Studies of the microwave hysteresis have shown that decoration (processing in ethanol or acetone) lowers the superconducting transition temperature. In the single crystal, after decorating it with DPPH by crystallization from an acetone solution, the value of T_c and the intensity of the EPR signal are markedly decreased although the effects of the vortex lattice are very pronounced. Apparently, this result is connected with the action of the acetone on the surface of the single crystal. Decoration by deposition of finely dispersed DPPH powder from ethanol gave good results. Figure 3 shows the temperature dependence of the hysteresis amplitude in this case. Despite the decrease of T_c from 92 K to 72.5 K and to 79.3 K (see Fig. 4), the maximum in $\delta(T)$ remains narrow and close to the measured value of T_c . We also observed that some decorated samples recovered their superconducting properties over the course of a week (see Fig. 4, 1-3). In other words, these processes taking place during decoration by deposition from ethanol are reversible.

In the case in which the external magnetic field is perpendicular to the surface of the single crystal, we discovered an abrupt broadening of the EPR line below T_c . Figure 4 shows the temperature dependences of the hysteresis amplitudes and the width of the EPR line in decorated single crystals of $\text{YBa}_2\text{Cu}_3\text{O}_{7-\delta}$ for this orientation. The complete correlation between the two curves for all of the samples shows that the observed broadening is connected with the transi-

tion to the superconducting state. Note that the growth of ΔB just below T_c is more abrupt than for the ceramic samples. The linewidth increases by a factor of more than 40 in the small temperature range $\Delta T \approx 4$ K, while for the ceramic samples of $\text{YBa}_2\text{Cu}_3\text{O}_{7-\delta}$ it grows by a factor of only 8 over the entire temperature range. Further observation of the growth of the linewidth for the single crystals, unfortunately, was impossible because of the low amplitude of the signal, which itself was due to the small quantity of DPPH deposited on the surface of the crystal.

The temperature behavior of the linewidth for parallel orientation of the external magnetic field is more complicated (see Fig. 5). The character of the dependence $\Delta B(T)$ varies as a function of how much the external scanning field differs from its resonance value ($\Delta B_{\text{up}} = B - B_r$). Figure 5 shows the dependence $\Delta B(T)$ below T_c for single crystals of $\text{YBa}_2\text{Cu}_3\text{O}_{7-\delta}$ for $\Delta B_{\text{up}} = 200$ and 1000 Oe. It can be seen that there are two maxima in each function. The first maximum, just below T_c , is connected with the superconducting transition of the entire crystal. The steepness of these maxima is greater for the case $\Delta B_{\text{up}} = 1000$ Oe than for a scanning sweep of 200 Oe. The maximum observed at 50 K is more difficult to interpret. However, the strong dependence of its peak value on ΔB_{up} allows us to associate it with flux pinning.

To estimate the influence of flux pinning on the EPR linewidth, we measured the linewidth for various ΔB_{up} . Figure 6 shows the corresponding dependences on the field ΔB_{up} for two different temperatures near the second maximum— $T = 55$ K and 65 K. The magnitude of ΔB was measured as the distance between the peaks in the EPR signal.

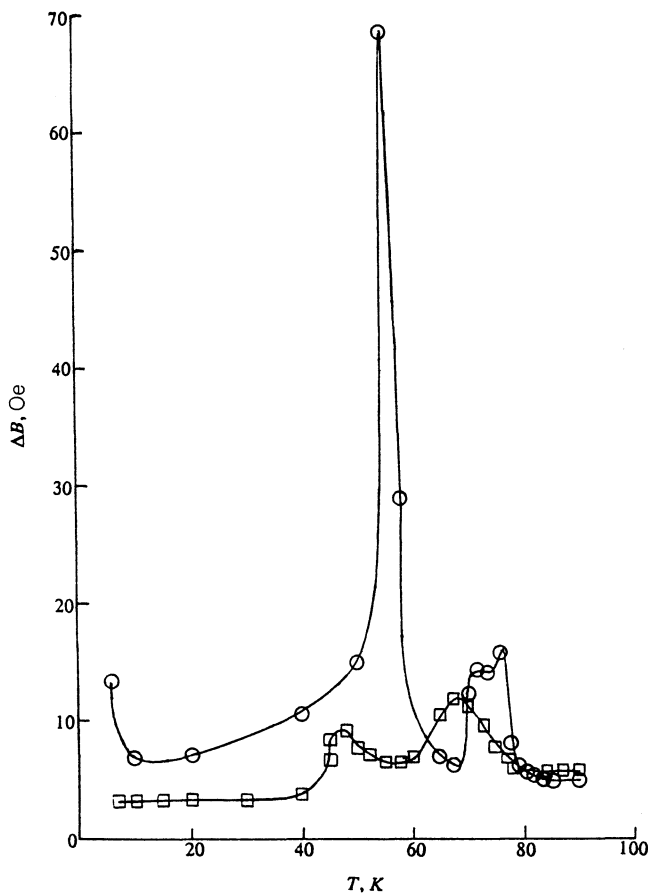


FIG. 5. Temperature dependences of the EPR linewidth for a single-crystal sample of $\text{YBa}_2\text{Cu}_3\text{O}_{7-\delta}$ for the external magnetic field oriented parallel to the crystal plane for maximum amplitude of the scanning field equal to 200 Oe (\square) and 1000 Oe (\circ).

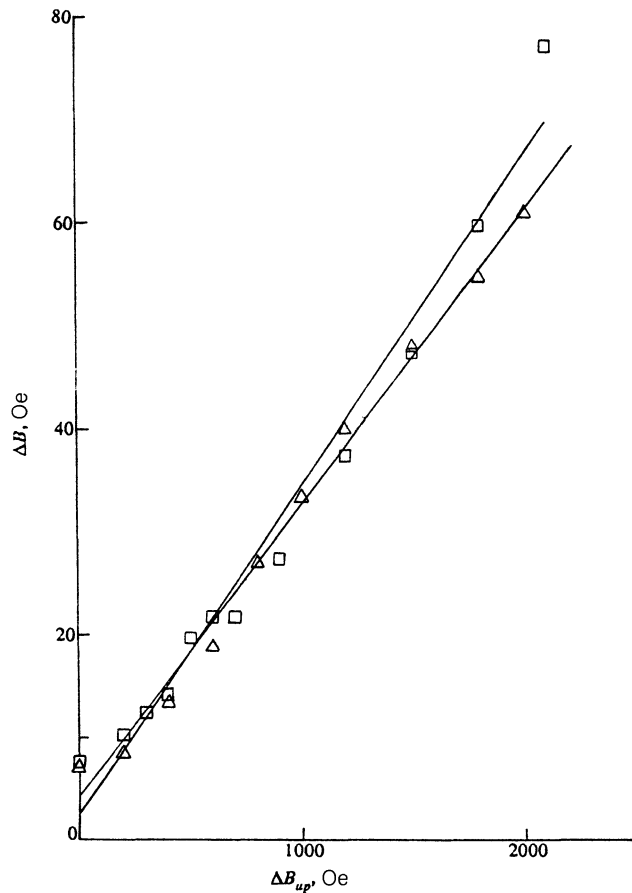


FIG. 6. Dependence of the width of the EPR signal for a single-crystal sample of $\text{YBa}_2\text{Cu}_3\text{O}_{7-\delta}$ for parallel orientation on the amplitude of the scanning field B_{up} for $T = 55$ K (Δ) and $T = 65$ K (\square).

The shape of the EPR signals in the samples which had been subjected to high fields (a large value of ΔB_{up}) varied greatly, acquiring a plateau-like distortion in the middle of the spectrum. The observed variation of the EPR spectrum is shown in Fig. 7. It should be noted that at large values of ΔB_{up} there is no significant shift of the resonance line.

Figure 8 shows a set of EPR spectra for the case in which the external magnetic field is oriented parallel to the plane of the $\text{YBa}_2\text{Cu}_3\text{O}_{7-\delta}$ single crystal. Variations of the shape of the spectrum are associated with rotation of the crystal plane by a small angle ($\sim 1^\circ$).

4. DISCUSSION

4.1. Ceramic samples

The absence of a strong spin-spin correlation in the system DPPH-superconducting surface makes it possible to treat it as a system of noninteracting magnetic spins, located in an inhomogeneous magnetic field. This picture is reminiscent of the situation which takes place in the NMR technique when studying vortex lattices. Pincus *et al.*,¹⁴ who were the first to account for the contribution of the vortex lattice to the NMR signal, made use of the following form:

$$(\overline{\Delta B^2})^{1/2} = \frac{\bar{B}}{\sqrt{4\pi}} \left(\frac{d}{\lambda} \right) \left[1 + \left(\frac{2\pi\lambda}{d} \right)^2 \right]^{-1/2} \approx \frac{\Phi_0}{\lambda^2 \sqrt{16\pi^3}}, \quad (2)$$

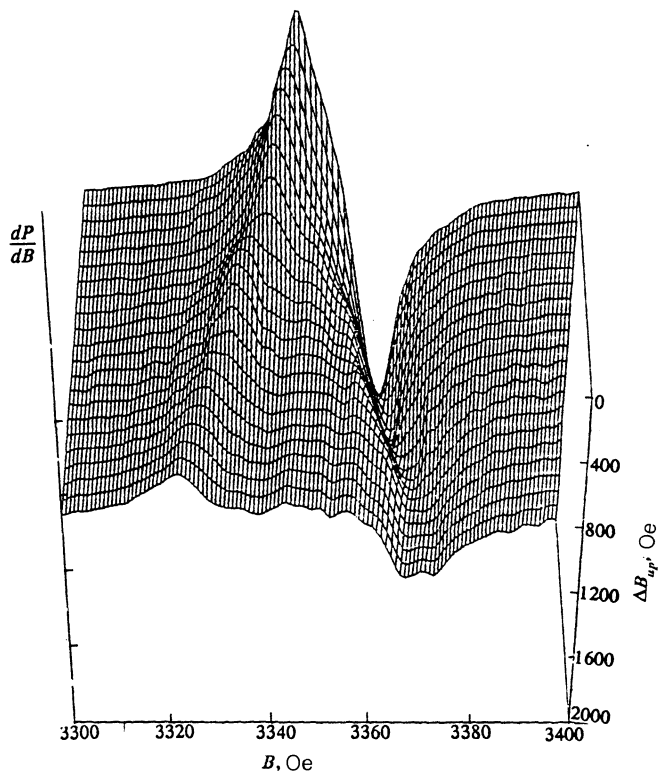


FIG. 7. Evolution of the shape of EPR signal for a single-crystal sample of $\text{YBa}_2\text{Cu}_3\text{O}_{7-\delta}$ as the amplitude of the scanning field increases.

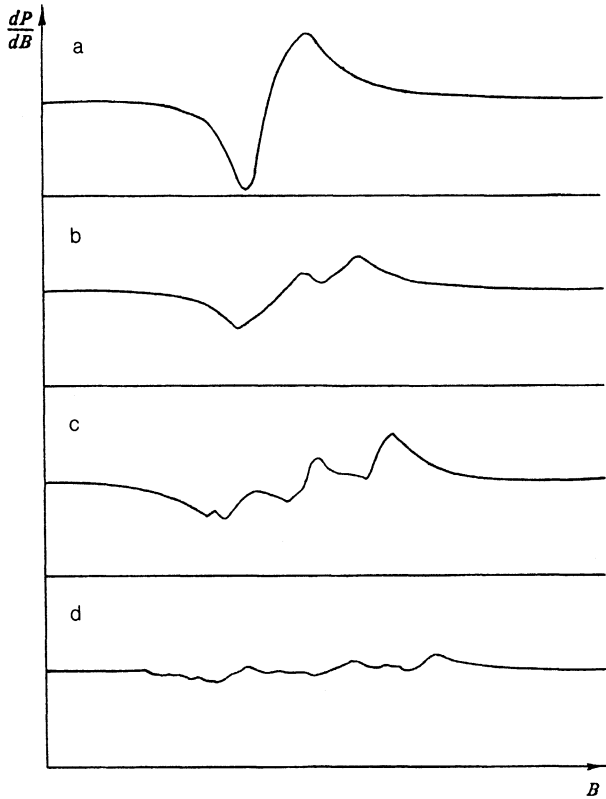


FIG. 8. Evolution of the shape of the EPR signal for a single-crystal sample of $\text{YBa}_2\text{Cu}_3\text{O}_{7-s}$ for stepped variation of the orientation of the external magnetic field in steps of 1° .

where d is the vortex lattice parameter in the square lattice approximation, \bar{B} is the external magnetic field, and $\Phi_0 = 2.068 \cdot 10^{-7} \text{ Oe} \cdot \text{cm}^2$ is the flux quantum.

The contribution of the vortex lattice to the broadening of the EPR line is given by the formula

$$\Delta B_s(T) = \sqrt{\Delta B_0^2(T) + \overline{\Delta B}^2(T)}, \quad (3)$$

where ΔB_s is the observed EPR linewidth, ΔB_0 is the linewidth due to internal relaxation processes in DPPH (see Fig. 1). We assume that there are no other mechanisms of broadening of the EPR signal from the DPPH probe besides those enumerated above.

Brandt^{27,28} has shown that for "dirty" superconductors with $\lambda \gg \xi$, where ξ is the coherence length, independent of the superconductivity mechanism, the simple London picture is valid and for a triangular lattice $\overline{\Delta B}^2$ can be calculated from the relations

$$\overline{\Delta B}^2 = 0,00371 \Phi_0^2 \lambda^{-4} \quad \text{for } b = \bar{B}/B_{c2} \leq 0,25, \quad (4)$$

$$\overline{\Delta B}^2 = 7,52 \cdot 10^{-4} (1 - b)^2 [1 + 3,9(1 - b)^2] \Phi_0^2 \lambda^{-4} \quad \text{for } b \geq 0,7. \quad (5)$$

The magnetic field necessary to record the EPR signal was less than 3.4 Oe and the condition $b < 0.25$ was fulfilled for temperatures $t = T/T_c \leq 0.9$, wherefore Eqs. (3) and (4) can be used to process the data.

For a more careful analysis of the observed behavior of

$\Delta B(T)$ we have proposed a qualitative model analogous to that developed for μ^+ SR experiments,²⁸ but with a cruder approximation.

To obtain the surface distribution of the local magnetic fields, we will consider an ideal square vortex lattice:

$$B_s(\mathbf{r}) = \sum_{i,j} B_{ij}(|\mathbf{r} - \mathbf{r}_{ij}|), \quad i, j = 1, 2, \dots, \quad (6)$$

where $B_{ij}(|\mathbf{r} - \mathbf{r}_{ij}|)$ is the field contribution from the vortex located at $\mathbf{r}_{ij} = (a_i, b_j)$. The experimental conditions, temperature range, and intensity of the magnetic field all taken together allow us to use the London limit of the solution of the Ginzburg-Landau (GL) equation.^{28,37} To calculate the magnetic contributions from the vortices, we used an approximate description of the magnetic field of a single vortex, which does not take account of the core:

$$B_{ij}(|\mathbf{r} - \mathbf{r}_{ij}|) = B^* \sqrt{\frac{\lambda}{|\mathbf{r} - \mathbf{r}_{ij}|}} \exp\left(-\frac{|\mathbf{r} - \mathbf{r}_{ij}|}{\lambda}\right). \quad (7)$$

Here \mathbf{r}_{ij} is the position vector of the vortex center. A modified value B^* of the magnetic field at the center of the core ($\mathbf{r} = \mathbf{r}_{ij}$) has been introduced in order not to reflect saturation in the case $\mathbf{r} \rightarrow \mathbf{r}_{ij}$ and $|\mathbf{r} - \mathbf{r}_{ij}| \ll \xi$, thereby making it possible to obtain agreement between Eq. (7) and the GL equation for all other distances ($|\mathbf{r} - \mathbf{r}_{ij}| \gg \xi$). Thus, the quantity B^* is another parameter that we need to estimate in order to get a reasonably good fit in the range $|\mathbf{r} - \mathbf{r}_{ij}| \leq \xi$. Note that these corrections can be considered more rigorously. However, this is not fundamental for the calculations of the local field distribution.

The insert in Fig. 9 shows an example of the two-dimensional $B_s(\mathbf{r})$ distribution obtained under the following experimental conditions: $d = 2000 \text{ \AA}$, $\lambda = 3000 \text{ \AA}$. This pattern is completely consistent with the result found from the exact solution of the Ginzburg-Landau equation.²⁹

The density of the local magnetic fields was calculated by summing the points within the limits of one vortex cell. (The magnetic field $B_s(\mathbf{r})$ has a unique value in these vortex cells). The corresponding curve $n_1(B)$ is plotted in Fig. 9. From the figure it is clear that high magnetic fields do not contribute to the broadening of the EPR line, since the right high-field limb of the curve $n_1(B)$ is quite far from the maximum of the curve, which is determined by the broadening process. Therefore, the assumption made above of the insignificant role of the values of magnetic field in the region $|\mathbf{r} - \mathbf{r}_{ij}| \leq \xi$ is reasonable.

Let us consider processes that change the resonance field of the EPR line at temperatures below T_c . Departing from the theoretically calculated curve $n_1(B)$, it is possible to determine the mean value of the local fields $\langle B \rangle$ which corresponds to an external magnetic field \bar{B} without diamagnetic shielding effects. The value of $\langle B \rangle$ obtained for $n_1(B)$ is greater than the field value corresponding to the maximum of $n_1(B)$ [$(B^{\text{max}} - \langle B \rangle)/B^* = 0.015$], which should shift the EPR line toward higher fields, where $\lambda(T)$ has a lower value. On the other hand, the diamagnetic shielding effect should shift the EPR line toward lower fields because the magnetic flux lines are "squeezed out" from the interior of the superconductor and the magnetic field intensity exceeds the external field intensity on the surface of the sample.

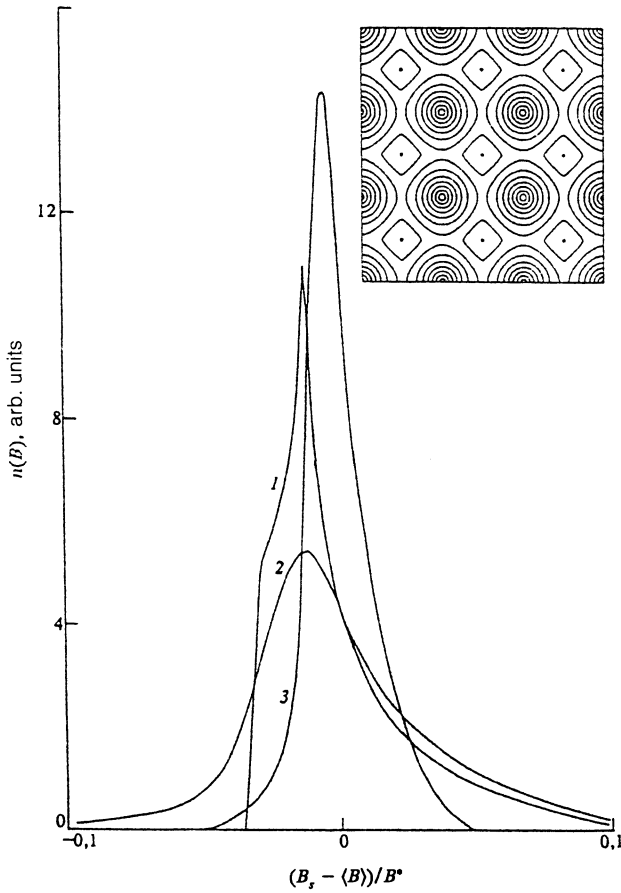


FIG. 9. Theoretical dependence of the density distribution function of the local magnetic fields on the surface of the superconducting sample. Curve 1—case of an ideal square vortex lattice, Curve 2—for a lattice with random (20%) displacements of the vortices from their equilibrium positions, Curve 3—the distribution function at the distance λ from the surface of the sample.

These two processes compete with one another and can both cause B_r to fall off as the temperature is lowered (see the inset in Fig. 1 for the ceramic $\text{YBa}_2\text{Cu}_3\text{O}_7$) and complicate the dependence of $B_r(T)$ (see the inset in Fig. 2 for $\text{Tl}_2\text{Ba}_2\text{Ca}_2\text{Cu}_3\text{O}_{10}$). This qualitative conclusion is in agreement with the temperature behavior of the resonance field for the superconducting alloys investigated in Ref. 38.

On the basis of the function $n_1(B)$ and the initial Lorentz lineshape $F(B)$ (with width ΔB_0) for DPPH, the expected EPR signal was calculated according to the following formula (see Fig. 10, curve 1):

$$F_1(\bar{B}) = \int_0^{B^*} dB' F(\bar{B} - B') n_1(B'). \quad (8)$$

This formula presupposes that at each point at which a paramagnetic center is located the external magnetic field \bar{B} and the local magnetic field are superposed due to the vortex lattice $n_1(B)$.

Figure 10 presents results of calculations of the EPR lineshape. The obtained line has an asymmetry of order 1.7. This quantity depends on the initial values of λ_s and d_s . This means that the asymmetry of the slopes of the distribution $n_1(B)$ and the low-field cutoff of this dependence are the main factors shaping the limbs of the EPR signal. The experimentally observed asymmetry of the EPR signals was

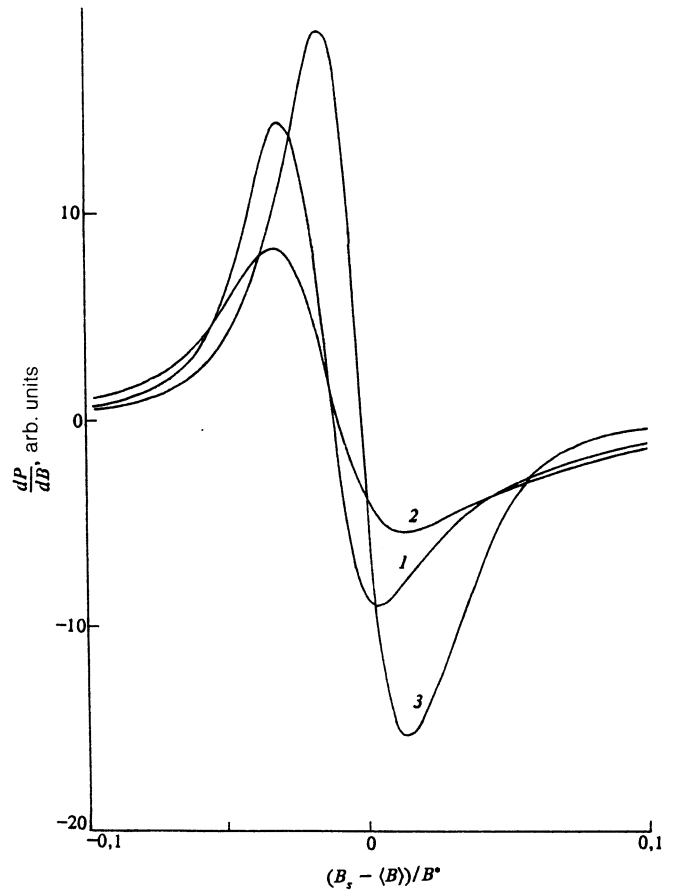


FIG. 10. Theoretical lineshapes of the EPR signals for calculated distribution functions of the local magnetic fields (see Fig. 9).

lower: 1.1 for $\text{YBa}_2\text{Cu}_3\text{O}_7$ and 1.0 for $\text{Tl}_2\text{Ba}_2\text{Ca}_2\text{Cu}_3\text{O}_{10}$.

The peak-to-peak EPR linewidth is determined for the most part by the relatively narrow interval of field strengths near the maximum of $n(B)$. At the same time, calculations predict that the shape of the peak strongly depends on the type of vortex lattice. A triangular lattice gives a narrower peak in the dependence of $n(B)$ than a square lattice or other distorted lattice.^{29,39} Thus, lattice irregularities due to pinning effects, etc. must be taken into account in the calculations.

The effect of strong surface pinning can be accounted for by introducing random shifts δr of the vortex centers in an ideal lattice from their equilibrium values.^{29,39} Figure 9 (curve 2) shows the calculated distribution $n_2(B)$ for the case of 20% deviation ($\delta r/r = 0.2$) of the flux lines from their equilibrium positions in an ideal square lattice. The corresponding lineshape (see Fig. 10, curve 2) is more symmetric and has greater broadening for the values of λ and B^* which were used in the calculation of curve 1.

In addition to pinning effects, there is one more important factor which must be taken into consideration in the calculations. In the decoration of the ceramic samples the paramagnetic centers are located at different distances from the surface of the superconductor because of the spread in the geometric dimensions of the DPPH grains. As a result, the magnitude of the local magnetic field varies but the local field distribution gradually smoothes out with distance from the surface and approaches its equilibrium form. We have assumed that the local field distribution tends toward the

equilibrium distribution exponentially with distance from the surface, so that at great distances the local magnetic fields should approach zero. The distribution $n_3(B)$ for this case is shown in Fig. 9 (curve 3). The lineshape is more symmetric and the linewidth narrower; however, the maximum in the curve $n_3(B)$ remains in the field region below the average field $\langle B \rangle$ (see Fig. 10, curve 3).

It is important to note that according to the foregoing discussion of the lineshape there are at least two factors which modify the value of $\lambda(T)$ determined on the basis of EPR data. On the one hand, irregularities in the vortex lattices caused by pinning effects cause $n(B)$ to be smeared out and, correspondingly, additional broadening of the EPR line. In this case the estimates of $\lambda(T)$ based on the dependence $\Delta B(T)$ will be smaller than the true values. On the other hand, the finite dimensions of the DPPH grains mask the inhomogeneous broadening of the EPR signal and cause the estimates of $\lambda(T)$ to exceed the true values. We believe that all these difficulties arise mainly as a result of the inadequate quality of the sample surface and quality of decoration.

In addition, because of the layered structure of the investigated high-temperature superconductors, the grains have a plate-like shape. Therefore a greater fraction of the DPPH grains fall onto the ab plane of the microcrystals and the obtained value of $\bar{\lambda}$ does not reflect complete averaging of λ over all orientations. This constitutes the difference between the given technique and bulk-sensitive techniques such as μ^+SR .

On the basis of formulas (1) and (2) and our experimental data on the temperature dependences $\Delta B(T)$ for the ceramic samples $YBa_2Cu_3O_7$ (Fig. 1) and $Tl_2Ba_2Ca_2Cu_3O_{10}$ (Fig. 2), we have obtained the temperature dependences of the penetration depth $\lambda(T)$ (see Fig. 11). For comparison, the figures also present the theoretical values of $\lambda(T)$, calculated according to the BCS model:³⁷

$$\lambda(T)^{-1} = \lambda(0)^{-1} \sqrt{1 - (T/T_c)^4}. \quad (9)$$

The dependence of $\lambda(T)$ obtained for the ceramic $YBa_2Cu_3O_7$ is in good agreement with the theoretical curve over the entire temperature range for $\lambda_0 \equiv \lambda(T=0) = 3500 \text{ \AA}$. The error in the determination of λ_0 was confirmed. The experimental and theoretical curves begin to deviate significantly when λ_0 deviates by 100 \AA . The obtained value of λ_0 is an overestimate since neither the geometric dimensions of the DPPH grains nor the presence of a superconducting layer on the surface of the sample was taken into account.

A similar behavior of $\lambda(T)$ was observed for the sample of the ceramic $Tl_2Ba_2Ca_2Cu_3O_{10}$, but with greater deviation in the intermediate temperature range from 50 to 100 K. This deviation can be explained by the presence on the surface of the sample of different superconducting phases with different T_c (80, 110, 120 K), which exist in the Tl-based superconducting samples. For this reason, the linewidth is observed to grow almost linearly with decreasing temperature down to helium temperatures. The best agreement between the experimental and theoretical curves for $\lambda(T)$ was obtained for $\lambda_0 = 3900 \text{ \AA}$. The additional broadening below 22 K can be ascribed to intrinsic broadening of the pure DPPH signal (see Fig. 1).

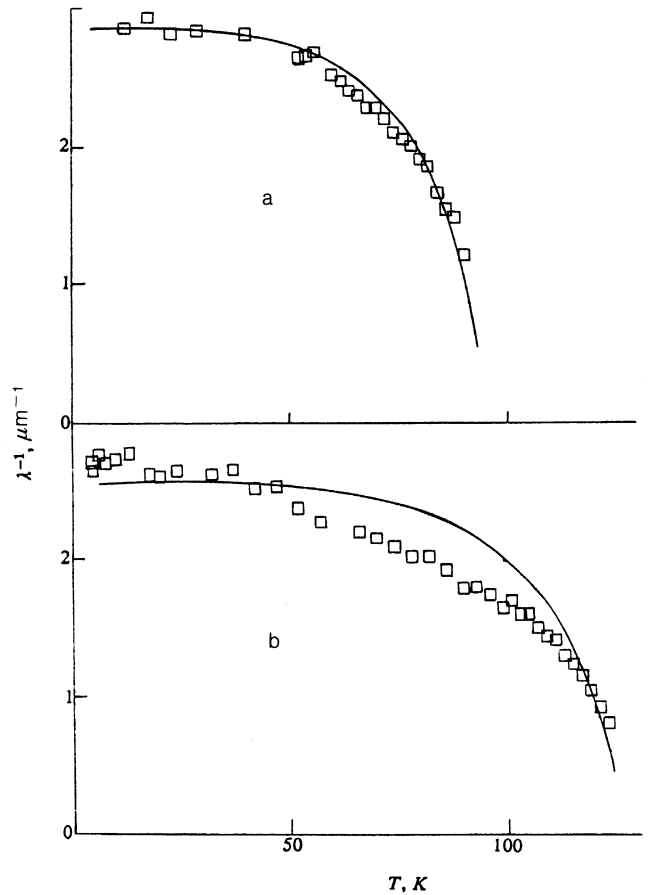


FIG. 11. Temperature dependence of the penetration depth $\lambda(T)$, extracted from the experimental data (see Figs. 1 and 2) and the corresponding theoretical dependence (solid curves), calculated according to the BCS model, for a sample of the ceramic $YBa_2Cu_3O_{7-\delta}$ (a) and the ceramic $Tl_2Ba_2Ca_2Cu_3O_{10}$ (b).

4.2. Single-crystal samples

4.2.1. Parallel orientation. Analysis of the experimental results obtained in the decorated superconducting samples revealed certain difficulties in the determination of the exact value of λ_0 , which are connected with the necessity of taking account of the distribution of the magnetic field in a granular sample. During the preparation of the sample the organic radical DPPH, while being deposited on the surfaces of the grains, falls into various intergranular cavities and therefore forms a set of microprobes in different configurations of the external magnetic field relative to the surface of the microcrystals. Moreover, besides the local magnetic fields as a result of the vortex lattices in the grains, the spectral parameters are also affected by the inhomogeneous magnetic field arising in the intergranular space due to the Meissner effect. Model experiments showed that the two effects superimpose, leading to a complicated behavior of the EPR linewidth below T_c .^{20,21} According to the theoretical model, the effects of the vortex lattice and Meissner shielding cannot be separated exactly for the case of superconducting ceramics.

Decoration of single-crystal samples is a convenient way of resolving the problem in a purely experimental way. In this case, on the one hand, the mutual configuration of the external magnetic field and the surface of the single crystal is clearly determined and, on the other, it is known with abso-

lute certainty that the DPPH is located on the ab surface of the single crystal.

In the case of the parallel configuration $\mathbf{H}_0 \parallel (ab)$, the magnetic inhomogeneity of the perpendicular cross section of the vortex lattice has no effect on the DPPH paramagnetic centers, since the Abrikosov vortices are lined up parallel to the surface. The magnetic inhomogeneity associated with Meissner shielding now becomes the main source of inhomogeneous broadening of the EPR signal. The temperature dependence of the EPR linewidth for the given configuration is shown in Fig. 5 for two values of the scanning field (200 Oe and 1000 Oe).

The influence of the sweep amplitude of the magnetic field on the scale of variations of the EPR linewidth (Fig. 5) indicates that there is a relation between the captured flux and the spectral characteristics. Figure 6 presents the experimental dependence of the EPR linewidth on the maximum intensity of the external magnetic field. The experiment was performed at two temperatures 55 and 65 K, chosen near the maximum of $\Delta B(T)$. Both dependences are well described by a linear law (see Fig. 6) with proportionality coefficient $K = \Delta B / \Delta B_{\text{up}} = 0.03$. According to Bean's model, flux capture by the superconducting crystal due to variation in the vortex density at the surface results in a proportional variation of the inhomogeneity of the local magnetic fields in the locations of the EPR probes, which in turn broadens the signal. Therefore, the coefficient $K = 0.03$ is an internal characteristic of the crystal which determines the pinning force. A fit of this dependence for $\Delta B_{\text{up}} = 0$ gives $\Delta B_{\text{res}} = 2.8$ Oe, which is in satisfactory agreement with the experimental value $\Delta B(55 \text{ K}) = 7$ Oe, allowing for intrinsic broadening of the DPPH signal.

Thus, the observed broadening of the EPR line in the parallel orientation can be said to be caused entirely by Meissner shielding with allowance for flux capacitance. The obtained experimental dependence makes it possible to estimate the contribution of diamagnetism to the linewidth in the parallel configuration, and in the perpendicular configuration $\mathbf{H}_0 \perp (ab)$ as well for the sample.

For ceramic HTSC samples decorated with DPPH, a correlation of the resonance field shift with the scanning amplitude of the magnetic field²⁰ and with the average grain diameter²⁴ was observed earlier. It is therefore logical to connect the peculiarities of the shift and the broadening of the EPR signal with inhomogeneities of the magnetic field in the intergranular space. Ravkin *et al.*²⁰ carried out experiments to determine the effect of diamagnetic shielding on the EPR linewidth. For DPPH deposited in the form of a small spot on a ceramic pellet of $\text{YBa}_2\text{Cu}_3\text{O}_7$ the following results were obtained: after increasing the magnetic field to 8600 Oe, the lineshift stood at $\Delta B_r = -60$ Oe. Then, after decreasing the field to zero, it increased to 10 Oe. Hence, the total scale of variation of the resonance fields in response to the application of a maximum scanning amplitude of 9 kOe was less than 70 Oe. On the basis of these results, the effects associated with inhomogeneous broadening due to diamagnetism are seen to be comparable with the effects of the vortex lattice in the decorated ceramic samples.

Using the experimental data from Ref. 20 (see Fig. 3 in Ref. 20—the temperature dependences of ΔB_r^{up} and ΔB_r^{down}), we calculated the dependence $\Delta B(T) = \Delta B_r^{\text{up}}(T) - B_r^{\text{down}}(T)$ (see Fig. 12). This latter depend-

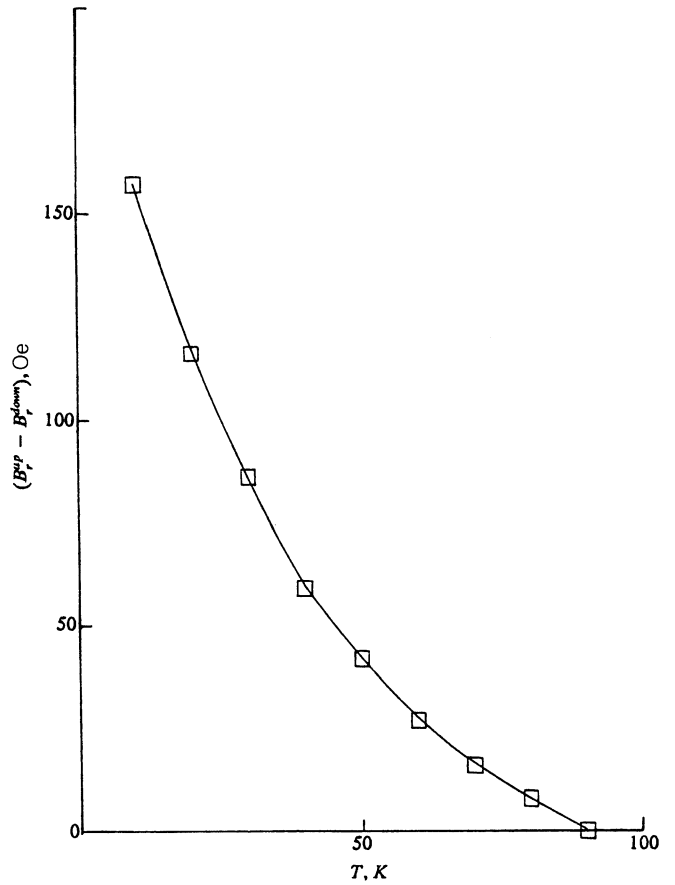


FIG. 12. Temperature dependence of the EPR linewidth due to the non-zero value of the sweep amplitude, calculated from the data in Ref. 20.

ence can be interpreted as the expected width of the signal as a result of flux capture for the ceramic sample $\text{YBa}_2\text{Cu}_3\text{O}_{7-\delta}$ after maximum scanning of the magnetic field. Here the value of $B_r^{\text{up}}(T)$ was determined after raising the magnetic field to 8600 Oe, and $B_r^{\text{down}}(T)$, after lowering it to zero. By comparing this dependence with the curve shown in Fig. 6 for the single crystal, we can see that the experimentally observed broadening effect is more strongly pronounced for the single-crystal sample (for $T = 55$ K the value $\Delta B = 400$ Oe is attained in the ceramic sample for scanning to 8600 Oe, while for the single crystal the same broadening is observed for scanning to 1300 Oe). Consequently, the observed broadening for the single-crystal sample cannot be completely explained by the Meissner effect. The only other broadening mechanism must be the appearance of the vortex lattice in the bulk of the superconductor; however, quantitative estimates have not been carried out since there is as of yet no supporting theoretical model.

Departing from the data shown in Fig. 6, we can estimate the effect of flux capture on the observed linewidth. In the experiment we scanned the field from 20 to 100 Oe, which caused additional broadening of the signal by not more than 4 Oe. Since the total linewidth for the various broadening factors is calculated according to Eq. (3), the maximum effect of flux capture is observed on lines of width 6 Oe and results in a broadening of the signal of not more than 50%. For other cases this effect is less significant.

4.2.2. Perpendicular orientation. In contrast to the case of parallel orientation, for perpendicular orientation of the

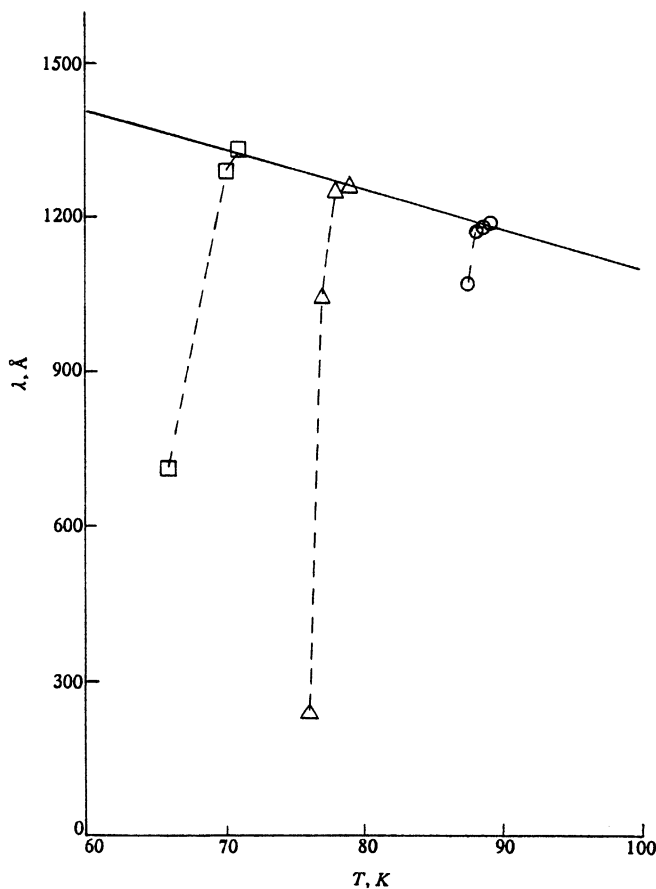


FIG. 13. Temperature dependence of penetration depth $\lambda(T)$, extracted from the experimental data (see Fig. 4).

external magnetic field relative to the surface of the single crystal the effect of the vortex lattice on the EPR signal is quite clear and well understood from the DPPH probe (see Section 4.1.). The quantitative estimates of $\lambda(T)$ for single crystals of $\text{YBa}_2\text{Cu}_3\text{O}_7$ are more correct than the quantitative estimates for the ceramic samples as a consequence of the better defined arrangement of the DPPH grains and the possibility of taking full account of the Meissner effect.

Figure 4 displays the temperature dependence of ΔB for single crystals of $\text{YBa}_2\text{Cu}_3\text{O}_7$. The abrupt broadening observed just below T_c (from 2 to 80 Oe within a temperature interval of 4 K) confirms that the contribution of the vortex lattice to the broadening of the EPR dominates the contribution of the Meissner effect.

In accord with this theory, in order to describe the results of the experiments on the ceramic samples on the basis of Eqs. (2) and (3), the experimental results on the EPR linewidth for the single crystals of $\text{YBa}_2\text{Cu}_3\text{O}_7$ (see Fig. 4) were converted into the temperature dependence of the penetration depth $\lambda(T)$ (see Fig. 13). Since the DPPH particles were deposited only on the ab plane of the single crystal, we can set $\lambda(T)$ equal to $\lambda_1(T)$. This constitutes the difference between the results obtained for single-crystal samples and those obtained for the ceramic samples, where a value averaged over all orientations $\bar{\lambda}(T)$ obtains.

The experimental data yielded the value of the penetration depth $\lambda_1 = 1200 \text{ \AA}$, which is in good agreement with data obtained by other techniques.

4.2.3. *Orientational effects.* As has been already said, for

$T < T_c$ and parallel orientation of the single crystal a single inhomogeneously broadened EPR line is observed; however, a small rotation of the crystal in the external magnetic field (less than 1°) produces an abrupt alteration in the shape of the signal (see Fig. 8): one rotation causes the signal to, as it were, duplicate itself. A second rotation causes another, third, signal to appear, and so on until the signal is completely smeared out.

This effect can be qualitatively explained if we take account of the anchoring or pinning of the vortex lattice to microdefects of the sample (pinning centers). In the presence of an external magnetic field, the vortices are stretched in the direction of this external field. After the crystal is rotated through some angle with respect to the external field the vortex lattice is partially restructured, i.e., some of the vortices, anchored to the pinning centers, remain oriented as before, and some reorient along the new direction. As a consequence, two maxima appear in the local field distribution function $n(B)$, i.e., two EPR signals appear with different "resonance" fields (see Fig. 8b). With each subsequent rotation the number of signals increases further, as was observed in the experiment (see Fig. 8c and d). Simultaneously the signal amplitude decreases. This happens as a result of a decrease in the number of vortices oriented in the given direction. Thus, the dependence of the signal amplitude on the rotation angle must be connected with the pinning force, but to obtain quantitative estimates it would be necessary to construct a theory of the observed effect.

5. CONCLUSION

By decorating the surface of samples of ceramic superconductors $\text{YBa}_2\text{Cu}_3\text{O}_7$ and $\text{Tl}_2\text{Ba}_2\text{Ca}_2\text{Cu}_3\text{O}_{10}$ with an EPR probe, we have obtained the temperature dependence of the magnetic penetration depth. The implemented analysis shows that contributions to inhomogeneous broadening, [note that $\lambda(T)$ is calculated from the magnitude of this broadening] come not only from the vortex lattice, but also from diamagnetic shielding, the dispersion of the DPPH, and distortions in the vortex lattice due to pinning effects. Local (i.e., one-sided, not encompassing the edges of the single crystal) decoration makes it possible to separate the contributions to the broadening of the signal from diamagnetic shielding and from vortex lattice effects since, by virtue of the layering of $\text{YBa}_2\text{Cu}_3\text{O}_{7-\delta}$, for parallel orientation of the crystal plane relative to the external field the main contribution to the broadening comes from diamagnetic shielding, and for perpendicular orientation, from the vortex structure. The observed magnitude of the broadening in the parallel orientation was at most 4 Oe. This means that diamagnetic shielding gives rise to less than 50% of the total broadening of the signal over the entire temperature range investigated. In the perpendicular orientation, the line broadens from 2 to 80 Oe when the temperature is lowered only 4 K below T_c . This means that the dominant contribution to the broadening comes from the vortex lattice and confirms the validity of determining the value of λ from it for ceramic samples.

Values of λ_0 have been obtained for the ceramic $\text{YBa}_2\text{Cu}_3\text{O}_7$ (3500 \AA) and for the ceramic $\text{Tl}_2\text{Ba}_2\text{Ca}_2\text{Cu}_3\text{O}_{10}$ (3900 \AA). The difference between the estimates of λ_0 obtained in the present paper and those obtained by other techniques can be explained by incomplete

averaging over all orientations as a result of the layered structure of the grains of the sample. The temperature dependence of the penetration depth in the ceramic samples is similar to the dependence $[1 - (T/T_c)^4]^{-1/2}$ predicted by BCS theory. From the data on the broadening of the EPR line in the perpendicular orientation of the single crystal of $\text{YBa}_2\text{Cu}_3\text{O}_7$, we have obtained the value $\lambda_1 = 1200 \text{ \AA}$, which is in good agreement with the results of other authors.

A qualitative model has been proposed which describes the influence of the vortex lattice on the formation of the EPR line, on the basis of which we have calculated the shape of the EPR line for the decorated samples.

The observed effect of multiplication of the number of EPR lines when the orientation of the single crystal changes slightly from the parallel is connected with pinning effects and in principle should make it possible to estimate the pinning force. We think that the technique of EPR-decoration of high-temperature superconductors which we have developed here can be a useful tool in the study of vortex lattices and the magnetic penetration depth.

We are grateful to A. I. Akimov and S. V. Naumov for providing samples. We also thank B. F. Gantmakher and V. M. Laptev for taking part in the discussion of results at various stages of this work and for moral support.

The present work was performed at the Center for EPR Spectroscopy of the Institute of Metal Physics within the framework of Project 90133 of the State Program on High-Temperature Superconductivity.

¹F. N. Gygax, B. Hitti, E. Lippelt *et al.*, *Europhys. Lett.* **4**, 473 (1987).

²G. Aeppli, R. J. Cava, E. J. Ansaldo *et al.*, *Phys. Rev. B* **35**, 7129 (1987).

³W. J. Kossler, J. R. Kempton, X. H. Yu *et al.*, *Phys. Rev. B* **35**, 7133 (1987).

⁴D. R. Harshmann, G. Aeppli, E. J. Ansaldo *et al.*, *Phys. Rev. B* **36**, 2386 (1987).

⁵W. J. Gallagher, T. K. Worthington, T. R. Dinger *et al.*, *Physica B* **148**, 228 (1987).

⁶P. Monod, B. Dubois, and P. Odier, *Physica C* **153-155**, 1489 (1988).

⁷J. R. Cooper, M. Petrávič, D. Drožić *et al.*, *Physica C* **153-155**, 1491 (1988).

⁸P. Peyrals, J. Rosenblatt, A. Robouton *et al.*, *Physica C* **153-155**, 1493 (1988).

⁹A. Schenk, *Physica C* **153-155**, 1127 (1988).

¹⁰D. R. Harshmann, L. F. Schneemeyer, F. Holtzberg *et al.*, *Phys. Rev. B* **39**, 851 (1989).

¹¹L. Krusin-Elbaum, R. L. Greene, F. Holtzberg *et al.*, *Phys. Rev. Lett.* **62**, 217 (1989); E. M. Jackson, S. B. Liao, J. Silvis *et al.*, *Physica C* **152**, 125 (1988); A. Umezawa, G. W. Crabtree, J. Z. Liu *et al.*, *Phys. Rev. B* **38**, 2843 (1988).

¹²P. Birrer, F. N. Gygax, B. Hettich *et al.*, *Physica C* **158**, 230 (1989).

¹³M. Mehring, F. Hentsch, H. J. Mattausch *et al.*, *Z. Phys. B* **77**, 355 (1989).

¹⁴P. Pincus, A. C. Gossard, V. Jaccarino *et al.*, *Phys. Lett.* **13**, 851 (1964).

¹⁵J. M. Delrieu, *J. Phys. F* **3**, 893 (1973).

¹⁶A. G. Redfield, *Phys. Rev.* **162**, 367 (1967).

¹⁷P. Thorel, R. Kahn, Y. Simon, D. Cribier *et al.*, *J. Phys.* **34**, 447 (1973).

¹⁸J. R. Clem, *J. Low-Temp. Phys.* **18**, 427 (1975).

¹⁹J. R. Cooper, C. T. Chu, L. W. Zhou *et al.*, *Phys. Rev. B* **37**, 638 (1988); D. W. Cooke, R. L. Hutson, R. S. Kwok *et al.*, *Phys. Rev. B* **37**, 9401 (1988).

²⁰B. Ravkin, M. Požek, and A. Dulčić, *Physica C* **170**, 166 (1990).

²¹B. Ravkin, T. A. Mahl, A. S. Bhalla *et al.*, *Phys. Rev. B* **41**, 769 (1990).

²²B. Ravkin, M. Požek, and A. Dulčić, *Solid State Comm.* **72**, 199 (1989).

²³Yu. N. Shvachko, A. A. Koshta, A. A. Romanyukha *et al.*, *Physica C* **174**, 447 (1991); Yu. N. Shvachko, A. A. Koshta, A. A. Romanyukha *et al.*, *Physica C* **197**, 27 (1992).

²⁴N. Bontemps, D. Davidov, P. Monod *et al.*, *Phys. Rev. B* **43**, 11512 (1991).

²⁵G. Plesch, F. Hanic, C. Friebe *et al.*, *Proc. of the 13th Conf. on Coordination Chemistry, 11-14 June 1991, Bratislava*, p. 233.

²⁶A. A. Romanyukha, Yu. N. Shvachko, and V. V. Ustinov, *Usp. Fiz. Nauk* **161**, No. 10, 38 (1991).

²⁷E. H. Brandt, *Phys. Rev. B* **37**, 2349 (1988).

²⁸E. H. Brandt and A. Seeger, *Adv. Phys.* **35**, 189 (1986).

²⁹E. H. Brandt, *J. Low-Temp. Phys.* **73**, 355 (1988).

³⁰V. A. Kostylev, N. M. Chebotaev, S. V. Naumov *et al.*, *Sverkhprovodimost' (KIAE)* **3**, 1385 (1990); A. A. Samokhvalov, N. M. Chebotaev, V. A. Kostylev *et al.*, *Fiz. Met. Metalloved.* **67**, 741 (1989).

³¹A. M. Portis, in: *Int'l. School of Material Science and Technol.*, 16th Course, ed. by J. G. Bednorz and K. A. Müller, Springer, Heidelberg, 1989.

³²A. Dulčić, B. Leontić, M. Perić *et al.*, *Europhys. Lett.* **4**, 1403 (1987); M. Perić, B. Ravkin, M. Prester *et al.*, *Phys. Rev. B* **37**, 522 (1988).

³³Yu. N. Shvachko, D. Z. Khuzainov, A. A. Romanyukha *et al.*, *Solid State Comm.* **69**, 611 (1989).

³⁴A. A. Romanyukha, Yu. N. Shvachko, V. Yu. Irkhin *et al.*, *Physica C* **171**, 276 (1990).

³⁵A. A. Koshta, A. A. Romanyukha, Yu. N. Shvachko *et al.*, *Sverkhprovodimost' (KIAE)* **3**, 338 (1990); A. A. Koshta, Yu. N. Shvachko, A. A. Romanyukha *et al.*, *Bull. Magnet. Res.* **12**, 89 (1990).

³⁶H. A. Blackstead, D. B. Pulling, P. J. McGuinn *et al.*, *Physica C* **174**, 394 (1991).

³⁷A. A. Abrikosov, *Fundamentals of the Theory of Metals*, Elsevier, Amsterdam, 1988.

³⁸S. E. Barnes, *Adv. Phys.* **30**, 801 (1981).

³⁹P. H. Kes, *Physica C* **153-155**, 1121 (1988).

Translated by P. F. Schippnick